Erschienen in: Nineteenth European Photovoltaic Solar Energy Conference : proceedings of the international conference held in Paris, France, 7 - 11 June 2004; Vol 1 / Hoffmann, W. et al. (Hrsg.). - München [u.a.] : WIP [u.a.], 2004. - S. 427-430. - ISBN 3-936338-14-0

HYDROGENATION OF MULTICRYSTALLINE SILICON – THE STORY CONTINUES

G. Hahn[1], D. Sontag[1], S. Seren[1], A. Schönecker[2], A.R. Burgers[2], R. Ginige[3], K. Cherkaoui[3], D. Karg[4], H. Charifi[4]
[1]University of Konstanz, Department of Physics, PO Box X916, 78457 Konstanz, Germany
[2]ECN Solar Energy, PO Box 1, 1755ZG Petten, Netherlands
[3]NMRC, Lee Maltings, Prospect Row, Cork, Ireland
[4]Institute of Applied Physics, University of Erlangen, Staudtstr. 7, 91058 Erlangen, Germany
Tel: +49-7531-88-3644, Fax: +49-7531-88-3895. Email: giso.hahn@uni-konstanz.de

ABSTRACT: Hydrogenation kinetics of defected mc Si materials has been investigated. For the first time deuterium originating from a hydrogen-rich PECVD SiN layer could be detected deep in the bulk of oxygen-rich material by SIMS after a firing step. A model for hydrogen diffusion is described, which is based on the monitoring of the overall O and C concentration, $[O_i]$, $[C_s]$, and vacancy concentrations in the as-grown wafer as well as after emitter diffusion. Trapping of hydrogen at oxygen precipitates can explain the observed D-profiles. Precipitation of oxygen is a function of as-grown $[O_i]$ and thermal pre-treatment. If $[O_i]$ is below a critical threshold, reduced precipitation leads to a low density of precipitates and deuterium concentration is at or below the SIMS detection limit. The concentration of vacancies does not seem to play a direct role in diffusion kinetics, but is linked to oxygen precipitation and can influence hydrogen concentration by dissociation of molecules, as proposed by other authors. A reduced oxygen content leads to faster diffusion of hydrogen which allows complete penetration of the whole wafer bulk in reduced passivation time and without additional traps competing with the atomic hydrogen.
Keywords: Multi-Crystalline - 1, Passivation – 2, PECVD - 3

1 INTRODUCTION

Defects in multicrystalline (mc) silicon wafers and solar cells can be passivated very effectively by in-diffusion of atomic hydrogen. In the current theory, the binding of the H-atom to Si in the vicinity of crystal defects (dislocations, grain boundaries, point defects, or precipitates and the surrounding strain field) can shift defect levels from a mid band gap position to a shallower position or to a level outside the band gap. This results in a reduced recombination activity of the underlying defect and thus increases lifetimes of the minority charge carriers. Although hydrogenation has been applied to mc Si for a long time, there seems to be a difference in the kinetics of mc Si in comparison to monocrystalline (mono) Si where much of the theoretical work has been carried out in the past. Van Wieringen and Warmoltz [1] could determine the diffusivity of H in mono Si, and this data was confirmed to be valid in a broad temperature range (see [2,3] for a summary). Diffusion of hydrogen in mc Si is much more complex because of the additional interaction with defects and not much is known about the kinetics, although mc Si solar cell processing relies a lot on hydrogenation during solar processing to increase efficiency.

This presentation will address some of the remaining issues in the hydrogenation process. This is a key feature for the fabrication of efficient solar cells made from defect-rich but cost-effective materials allowing a reduction in W_p-costs.

2 EXPERIMENTAL - HYDROGENATION

For this study two methods for hydrogenation have been used: (a) deposition of a hydrogen-rich SiN layer by remote plasma-enhanced chemical vapour deposition (PECVD) with subsequent firing to release the H-atoms into the Si bulk, (b) microwave-induced remote hydrogen plasma (MIRHP) passivation [4]. For both methods significant increases in carrier lifetime could be demonstrated for mc Si material [5,6]. But up to now there exists no direct proof of the hydrogen in the mc Si bulk after PECVD SiN deposition followed by firing, although it could be detected recently in mono Si in concentrations around 10^{14} cm^{-3} using a method with markers [2].

As H is common in the SIMS measurement ambient, it is usually replaced by D to increase the detection limit. For PECVD deposition we used ND_3 instead of NH_3 and for MIRHP a D_2 gas flow instead of H_2. A similar approach was chosen in a recent study of PECVD hydrogenation in mc Si, but no D could be detected in the Si bulk [7]. For high [O] materials D-profiles could be obtained using MIRHP [8].

In our investigation, samples were bevelled after hydrogenation and secondary ion mass spectroscopy (SIMS) was applied to determine the D concentration [D]. In this way deep profiles can easily be measured by tracking the bevelled surface with the Cs ion beam and calculating the depth via the bevel angle.

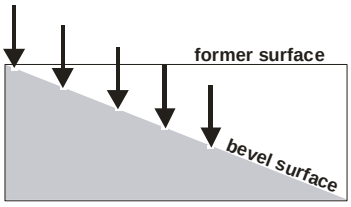

Figure 1: Bevelled sample for SIMS measurement.

3 EXPERIMENTAL - MATERIALS

For ribbon silicon pronounced lifetime increases after hydrogenation could be demonstrated [5,6] due to the relatively high amount of crystal defects present. Therefore, it should be a material well suited for the detection of hydrogen. On the other hand MIRHP D-profiles could only be detected in ribbon growth on substrate (RGS) silicon with a high [O], therefore we have chosen p-type materials with comparably high [O] for the SIMS analysis. The four RGS samples chosen

(1 Ωcm) differ only in their [O] due to modifications in the crystallisation ambient, the other defect concentrations present ([C], grain size, dislocation density, etc.) remain constant. Sample 2 has the same overall [O] as sample 1, but due to O-precipitation directly after crystallisation at temperatures >1000 °C for 1 h the interstitial oxygen concentration [O_i] is lower (measured by Fourier-transformed infrared spectroscopy, FTIR). The String Ribbon (SR, 3 Ωcm) sample was chosen as a reference representing low [O] material.

Table I: Samples used in the SIMS experiments. [O] and [C] from SIMS measurements, as-grown [O_i] from FTIR. No calibration between both methods has been applied.

No.	Material	[O] [cm^{-3}]	[O_i] [cm^{-3}]	[C] [cm^{-3}]
1	RGS	$3\text{-}4\cdot10^{18}$	$2.9\cdot10^{18}$	$2\text{-}3\cdot10^{18}$
2	RGS	$3\text{-}4\cdot10^{18}$	$<10^{18}$	$2\text{-}3\cdot10^{18}$
3	RGS	$2\cdot10^{18}$	$0.75\cdot10^{18}$	$2\text{-}3\cdot10^{18}$
4	RGS	$0.7\cdot10^{18}$	$0.3\cdot10^{18}$	$2\text{-}3\cdot10^{18}$
5	SR	$0.2\cdot10^{18}$	$<10^{17}$	$4\cdot10^{17}$

4 SIMS ANALYSIS - PECVD

Samples were diffused in an open-tube furnace at 850 °C for 20 min using $POCl_3$. Afterwards deposition of 75 nm SiN was performed in a remote PECVD system using SiH_4 and ND_3 in a ratio of 1/1.6 resulting in a refractive index n of 2.1-2.2. Samples were fired in a belt furnace using standard industrial-type co-firing conditions with the wafers exposed to temperatures >700 °C for about 10 s. Results of the following SIMS measurements for [O] and [D] after bevelling are shown in Fig. 2. [O] remains constant throughout the bulk with some variations at the edge of the bevel due to breakage.

For [D] only counts/s and no absolute concentrations have been obtained, as no standard was available (spot size was 30·30 µm and acquisition time 1 s per measurement point). Nevertheless, for the first time D-profiles after PECVD deposition and firing could be measured by SIMS for samples 1, 2, and 3. A high [O] leads to high [D] near the surface (1) and a steeper profile (1 as compared to 3). Comparing samples 1 and 2 a slightly steeper profile is observed for sample 1 with higher as-grown [O_i]. This is in agreement with results using MIRHP [8].

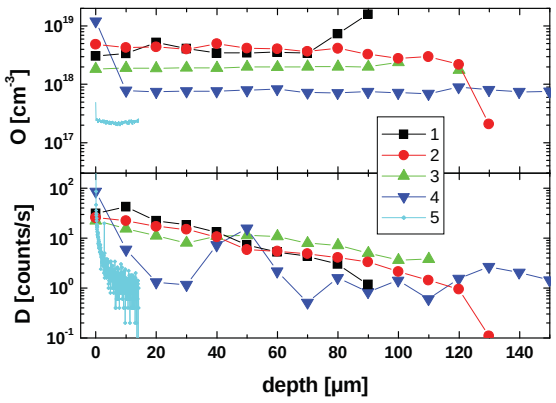

Figure 2: Oxygen and deuterium profiles of the PECVD samples (Table I) as measured by SIMS.

Samples 4 and 5 with [O] <10^{18} cm^{-3} lead to [D] in the range of the detection SIMS limit (1-2 counts/s). The hump at 40-50 µm depth for sample 4 coincides with a grain boundary, indicating that D might be trapped at the defects present in the grain boundary. The SR sample was not bevelled.

5 SIMS ANALYSIS - MIRHP

Hydrogenation using the MIRHP method was carried out on 3 RGS solar cells without antireflection coating originating from the same wafer (with [O] and [O_i] comparable to sample 2 from Table I). Passivation temperature was held constant at 450 °C, passivation time was 5, 10, and 24 h respectively. Samples were bevelled and D-profiles determined using SIMS (Fig. 3).

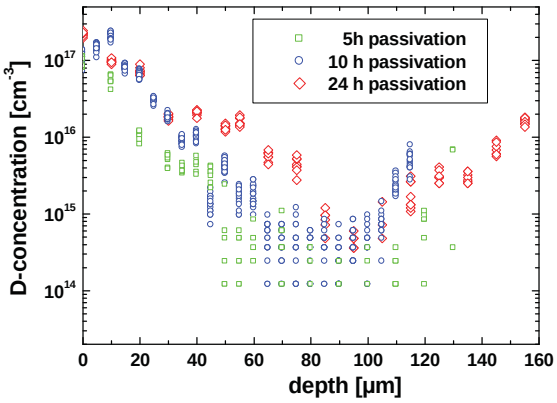

Figure 3: Deuterium profiles after MIRHP passivation at 450 °C as measured by SIMS.

Even the long passivation time of 24 h is not sufficient to detect D throughout the whole bulk. A symmetrical shape of the profile is observed as with the MIRHP technique D diffuses from both surfaces (emitter and Al-covered backside) into the sample. The slope of the profile and the low penetration depth again indicate a trapping mechanism during D-diffusion.

6 RETENTION OF HYDROGEN

Another way to measure the diffusivity of H in mc Si can be realized by annealing experiments. For this study we have chosen 4 solar cells, which have been completely hydrogenated using MIRHP. After IV measurement cells have been annealed for 15 min at a given temperature and IV was measured again. As a next step annealing was carried out at elevated temperature again followed by IV measurement, and so on. The results shown in Fig. 4 indicate that dissociation of H from the defect site is dependent on as-grown [O_i]. For the Edge-defined Film-fed Growth (EFG) cell with the lowest [O_i] in the same range as for the SR sample from Table I dissociation already starts after an anneal at 350 °C, whereas for the samples with highest [O_i] short circuit current density J_{sc} is stable up to 450 °C. Internal quantum efficiency measurements carried out in parallel prove that J_{sc} is decreased due to a lower red response indicating a drop in diffusion length while the blue

response remains constant [9]. Again it can be shown that a higher [O_i] slows down diffusivity in mc Si.

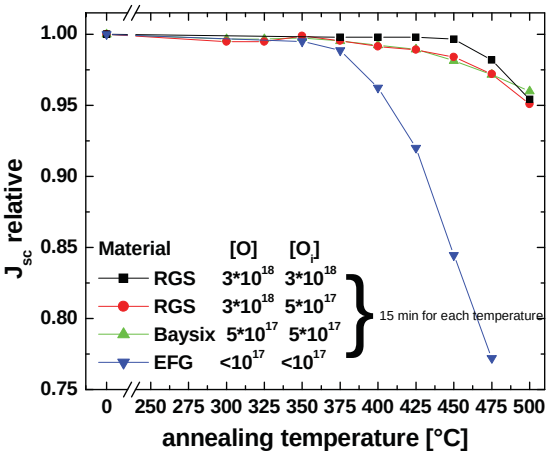

Figure 4: Annealing experiments for hydrogenated solar cells with different [O] and as-grown [O_i].

7 MODELLING OF THE MIRHP PROFILES

We tried to model the obtained D-profiles after MIRHP passivation (Fig. 3). Two types of diffusion are described in literature: free diffusion (error function) and trap-assisted diffusion (exponential). Assuming only free diffusion with the diffusion constant *D* as determined in [1] for mono Si, D-profiles would result in an almost horizontal line. Even by drastically reducing the diffusion constant the shape of the profiles can not be modelled assuming the same *D* for all samples. On the other hand, a diffusion mechanism relying on trapping without releasing the trapped D-atoms would result in an exponential decay of [D] as shown in Fig. 5. The shape of the measured profiles can only be simulated by assuming a mixture of free and trap assisted diffusion (compare with [10]).

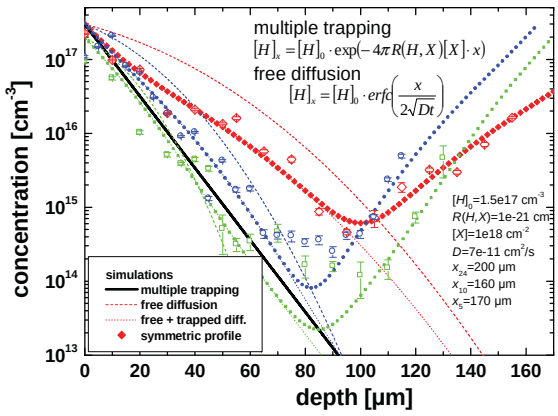

Figure 5: Empirical fits to the obtained MIRHP diffusion profiles (Fig. 3) with a set of diffusion parameters under the assumption of a mixture of trap-assisted and free diffusion with an effective diffusion constant *D*. Passivation times: 5 h (squares), 10 h (circles), 24 h (diamonds).

An empirical fit for a given set of diffusion parameters capture cross section *R(H,X)* of a trap *X*, trap concentration *[X]*, concentration at the surface $[H]_0$, and *D* in dependence of the depth *x* is shown in Fig. 5 by a superposition of the two diffusion mechanisms. Mean values and standard deviations are given as error bars for the points already shown in Fig. 3. The assumed effective diffusion constant at 450 °C of $7 \cdot 10^{-11}$ cm^2/s is several orders of magnitude lower than the one calculated from [1] ($4 \cdot 10^{-6}$ cm^2/s). An explanation for this discrepancy can be given when the time is taken into account during which the D-atom is trapped. Together with the free diffusion between the release from one trap and the recapture at the next one an effective diffusion constant results which can be significantly lower as the one in defect free mono Si without trapping. Note that in the formula for the trap assisted diffusion only the product of *R(H,X)·[X]* is responsible for the shape of the profile.

8 VACANCY CONCENTRATION

It is known from literature that the concentration of vacancies might influence H-diffusivity in silicon. Vacancies can assist in cracking hydrogen molecules in atomic hydrogen [11], and a mechanism for an increased diffusivity of H via a vacancy-hydrogen complex has been discussed [12]. It could be assumed that there is a link between high [O_i] and low [vac]. Therefore, vacancy concentrations [vac] have been measured using the Pt method [13,14] to check if a low [vac] is responsible for the slowed down diffusion of H or D. [vac] as well as [O_i] and [C_s] (FTIR) for samples of Table I in the as-grown state (1, 3, and 4) and after $POCl_3$ diffusion and SiN deposition (1-4, no firing) are shown in Table II.

Table II: [vac], [O_i], and [C_s] for samples listed in Table I and used for PECVD SIMS analysis in the as-grown state and after $POCl_3$ diffusion and SiN deposition.

	as-grown			after $POCl_3$, SiN		
	[vac] [10^{12} cm^{-3}]	[O_i] [10^{18} cm^{-3}]	[C_s] [10^{18} cm^{-3}]	[vac] [10^{12} cm^{-3}]	[O_i] [10^{18} cm^{-3}]	[C_s] [10^{18} cm^{-3}]
1	<1	2.9	2.6	<1	0.4	0.9
2		<1		10	0.4	1.5
3	20	0.75	3.1	<1	0.3	2.7
4	20-50	0.3	2.7	20-30	0.3	2.8

As-grown [vac] for the oxygen-rich RGS samples can be in the same range as measured for materials with low [O_i] like EFG [13], so [vac] is not a function of as-grown [O_i] alone. All RGS samples in the as-grown state reveal the same high [C_s]. A decrease in [vac] between the as-grown state and after $POCl_3$ diffusion and SiN deposition is most pronounced when there is a reduction in [O_i] as well (sample 3). As a change in [O_i] is the result of O-precipitation during the high temperature diffusion step, it is important to take into account the mechanisms for O-precipitation. Precipitation rate of O is a function of both [O_i] as well as [C_s]. A high [C_s] as present in all RGS samples enhances O-precipitation as long as the overall [O] is not below a certain threshold in the range of $5 \cdot 10^{17}$ cm^{-3} [15]. So the reduction in [vac] after diffusion can be explained by O-precipitation known to create self

interstitials. On the other hand, hydrogen diffusion in EFG is much faster as in sample 2 despite of the same [vac] after $POCl_3$ diffusion [13]. This indicates that hydrogen diffusivity is not directly linked to [vac].

9 DISCUSSION

Deduced from the results presented above, a consistent model can be derived. H can be trapped at oxygen precipitates like New Donors formed in the temperature range between 600-900 °C where it is known to reduce recombination strength by passivation [16]. H (or D) can only be detected when O-precipitates exist in sufficient concentration. These are present mainly in samples 1, 2, and 3. Precipitates for sample 2 are larger because they are formed at higher temperatures (>1000 °C). Their concentration is therefore lower. As H might interact with the O-precipitate via its surface, the reduced surface area for precipitates in sample 2 (lower concentration of large precipitates with the same overall [O]) can be responsible for the faster diffusion as compared to sample 1. The larger the surface area of the precipitates, the more H can be trapped, and the measured profile gets steeper. If [O_i] in the as-grown state is below a certain concentration, O-precipitation at high temperatures is slowed down even in the presence of high [C_s]. This explains the strongly decreased [D] for samples 4 and 5.

In this model the reduced H diffusivity in the bulk of materials with high [O] is not directly coupled with the [vac], but [vac] is influenced by precipitation of interstitial oxygen. A reduced [vac] due to generation of interstitials or absorption of vacancies during O-precipitation is therefore only an indirect marker of the reduced diffusivity of H. This does not question the ability of vacancies to create more atomic hydrogen by cracking of H_2 molecules, which might lead to a higher H-concentration, especially at the wafer surface.

MIRHP passivation is generally applied in a lower temperature regime (300-450 °C). Here the retention of hydrogen at the traps is more pronounced as compared to hydrogenation via PECVD SiN and firing. Typical activation energies for dissociation of hydrogen from defects are in the range of 2-3 eV, corresponding to temperatures of around 400 °C [17]. Consideration of trapping is therefore even more important and can explain the steep profiles measured even after long passivation times. First results for determination of the penetration depth of deuterium after MIRHP passivation of 1 and 10 h at 350 °C in mono Si samples with trap densities of ~10^{16} cm^{-3} according to the method proposed in [2] indicate depths <50 µm for both FZ and Cz [18]. More research will be carried out in this direction.

The reduced [O_i] led to lifetimes between 4-5 µs after hydrogenation in RGS wafers corresponding to sample 4 as compared to maximum values around 1 µs for hydrogenated wafers comparable with samples 1 and 2. In addition, this could be reached by reducing passivation time from >10 h to 1 h.

10 SUMMARY

For the first time D-profiles after deposition and firing of a PECVD SiN layer could be presented in mc Si material. [D] and the shape of the profiles depend on oxygen concentration. Higher [D] and steeper profiles due to trapping are observed in material with large amount of O-precipitates, which could be shown by comparing [O], [O_i], [C], and [C_s] in the as-grown state and after emitter diffusion. [vac] itself seems not to play the leading role in hydrogen diffusion kinetics, but is strongly linked to O-precipitation.

11 ACKNOWLEDGEMENTS

We like to thank M. Stavola for stimulating discussions and A.M. Gabor for SR material supply. Part of this work was supported by the EC in the frame of the RGSells project (ENK6-CT2001-00574) and by the German BMU in the frame of the ASIS project (0329858J).

12 REFERENCES

[1] A. Van Wieringen, N. Warmoltz, Physica 22 (1956) 849
[2] M. Stavola, F. Jiang, A. Rohatgi, D. Kim, J. Holt, H. Atwater, J. Kalejs, Proc. 3rd WC PEC, Osaka 2003, 909
[3] M. Stavola, in Properties of Crystalline Si, edited by R. Hull (INSPEC, London, 1999) 511
[4] M. Spiegel, P. Fath, K. Peter, B. Buck, G. Willeke, E. Bucher, Proc. 13th EC PVSEC, Nizza 1995, 421
[5] V. Yelundur, A. Rohatgi, J.-W. Jeong, A.M. Gabor, J.I. Hanoka, R.L.Wallace, Proc. 28th IEEE PVSC, Anchorage 2000, 91
[6] G. Hahn, W. Jooss, M. Spiegel, P. Fath, G. Willeke, E. Bucher, Proc. 26th IEEE PVSC, Anaheim 1997, 75
[7] H.F.W. Dekkers, S. De Wolf, G. Agostinelli, J. Szlufcik, T. Pernau, W.M Arnoldbik, H.D. Goldbach, R.E.I. Schropp, Proc. 3rd WC PEC, Osaka 2003, 983
[8] G. Hahn, P. Geiger, P. Fath, E. Bucher, Proc. 28th IEEE PVSC, Anchorage 2000, 95
[9] T. Pernau, G. Hahn, M. Spiegel, G. Dietsche, Proc. 17th EC PVSEC, Munich 2001, 1764
[10] B.L. Sopori, Y. Zhang, R. Reedy, Proc. 29th IEEE PVSC, New Orleans 2002, 222
[11] S.K. Estreicher, J.L Hastings, P.A. Fedders, Phys. Rev. B 57(20) (1998) R12 663
[12] B.L. Sopori, X. Deng, J.P. Benner, A. Rohatgi, P. Sana, S.K. Estreicher, Y.K. Park, M.A. Roberson, Solar Energy Materials and Solar Cells 41/42 (1996) 159
[13] D. Karg, G. Pensl, M. Schulz, Proc. 3rd WC PEC, Osaka 2003, 1112
[14] D. Karg, H. Charifi, G. Pensl, M. Schulz, G. Hahn, Proc. 19th EC PVSEC, Paris 2004, in press
[15] Q. Sun, K.H. Yao, J. Lagowski, H.C. Gatos, J. Appl. Phys. 67(9) (1990) 4313
[16] D. Karg, A. Voigt, J. Krinke, C. Hässler, H.-U. Höfs, G. Pensl, M. Schulz, H.P. Strunk, Solid State Phenomena 67-68 (1999) 33
[17] H.J. Möller, Semiconductors for Solar Cells (Artech House, Boston, 1993) 148
[18] W. Tang, M. Stavola, G. Hahn, unpublished results